Int. J. Electrochem. Sci., 12 **(2017)** 4370 – 4383, doi: 10.20964/2017.05.80

International Journal of ELECTROCHEMICAL SCIENCE
www.electrochemsci.org

Electrochemical Reduction of Nitrate on Different Cu-Zn Oxide Composite Cathodes

Shengxiang Yang[1], *Lizhang Wang*[1,*], *Xinmei Jiao*[1], *Peng Li*[2]

[1] School of Environment Science and Spatial Informatics, China University of Mining and Technology, Xuzhou City, Jiangsu 221116, PR China;
[2] School of Water Resource & Environmental Engineering, East China Institute of Technology, Nanchang, Jiangxi 330013, PR China
[*]E-mail: wlzh0731@126.com

Received: 4 January 2017 / *Accepted:* 17 March 2017 / *Published:* 12 April 2017

The scanning electron microscope (SEM), energy dispersive spectroscopy (EDS) and X-ray diffraction (XRD) techniques were used to investigate the physic-chemical properties of the base metal cathodes of Ti/CuO, Ti/Cu_5ZnO_x and Ti/$CuZn_5O_x$ prepared by thermal decomposition method. And the electrode performances were evaluated by linear sweep voltammetry (LSV) tests in alkaline solution and nitrate reduction by a membrane electrochemical cell. The SEM images and XRD patterns depict the prepared cathodes possess abilities of electrode area expansion and the oxide composite could be bound together with metal elements in nanoscale. The results during nitrate reduction indicate its removal relies on the potential and higher current density is beneficial to rapid nitrate conversion. In addition, the Ti/Cu_5ZnO_x is superior to others two materials via its inhibition of hydrogen evolution reaction: at 20 mA/cm^2, the nitrate removal efficiency of 92.3% and reduction selectivity S_x for N_2 generation of 33.7% were achieved after 6 h electrolysis, which approximates the performances of noble metals. Moreover, the nitrate removal is highly dependent of the quantity of active sites of the cathodes and zinc could offer active sites for intermediate N-species degradation, which could be directly confirmed by calculation of reaction rate constants through LSV tests. The mechanism is valid to for exploring possibility of high electroactivity not only on Cu-Zn oxide composite but also on other base element modified electrodes during nitrate reduction in alkaline solution.

Keywords: Thermal decomposition; Cu-Zn oxidize composite cathodes; Electrochemical process; Nitrate reduction

1. INTRODUCTION

Nitrate is a harmful pollutant that is restricted to be discharged into water bodies due to its risk both to aquatic ecosystems and human health [1, 2]. Hence, effective removal of nitrate becomes a central issue addressed with these problems. Many methods such as biological and physic-chemical processes have been reported by numerous publications [3-6]. Although considerable results were

achieved in these works, obvious drawbacks include lower reduction kinetics and byproduct generation related to the biological denitrification [3], as well as production of concentrated waste by the ion exchange [6], reverse osmosis [5] and electrodialysis [4]. All of those largely increase capital investment and operating cost, which hinder widely industrial application of these techniques. As a result, technology with higher efficiency and faster kinetics still should be developed to obtain complete conversion of nitrate to nitrogen gas (N_2).

Electrochemical method is considered to be another feasible way for efficient nitrate degradation. This process attracts much attentions and most study so far has focused on the efficiency of conversion of nitrate to N_2 on the electrode materials. To date, many researchers have reported that noble metals such as rhodium (Rh) [7] and palladium (Pd) [8, 9] exhibit excellent conversion of nitrate to dinitrogen; however, these kinds of elements are so scarce and costly that largely increase the operating cost of nitrate elimination, which strongly limits their field application. Aiming to decrease capital investment, performances of base metals including Fe [10], Sn [11, 12], Ti [10, 13], Cu [14] and Ni [15] as monometallic cathodes were investigated in detail. Among these, Cu has been proven to be a highly efficient promoter for nitrate reduction both in acidic and neutral media, and the products are N_2, nitrite or ammonia that determined by the applied potentials [16]; but the reaction efficiency would decrease due to electrode passivation caused by hydride formation after a long-period operation [17]. Though bimetallic alloys e.g. Cu-Ni [18], Cu-Sn [19] and Cu-Zn [20, 21] as cathodes can enhance nitrate reduction, the performance stability is still a central problem faced to these materials. Recently, CuO has been introduced into selective reduction of NO and maybe it could be used as a potential catalyst for NO_3^- reduction by combine with some oxidizes (e.g. CeO_2, MnO_2) [22-24]. However, to our knowledge there is little literature published on the employment of Cu-Zn oxide composite as cathode for the nitrate reduction. In addition, most of researchers have focused on performance of bimetallic alloys in the nitrate reduction, and none is associated with the discussion on the competitive adsorption between OH^-, H_{ads} and N-species at surface active sites or evaluation of the influence of solution pH to surface active sites on the various elements.

In this study, the objective was to discuss the performance of various Cu-Zn oxidize composite cathodes in the nitrate reduction and to determine the effect of solution pH to active sites on the surface of various elements. The scanning electron microscope (SEM), energy dispersive spectroscopy (EDS) and X-ray diffraction (XRD) were used to analyze the physic-chemical properties of the electrodes. The electro-catalytic activity and selectivity were assessed through linear sweep voltammetry (LSV) measurement and nitrate reduction in a membrane electrochemical cell. In addition, the degradation pathway and mechanisms for nitrate conversion on the three cathodes were discussed in detail.

2. EXPERIMENTAL SECTION

2.1. Chemicals

The chemicals in analytical pure containing $Cu(NO_3)_2{\cdot}3H_2O$, $Zn(NO_3)_2{\cdot}6H_2O$, ethanol, HNO_3, Na_2SO_4, NaOH, $NaClO_4$ and $NaNO_3$ were purchased from Sinopharm Chemical Reagent Co., Ltd (China). The nitrate solutions were prepared by deionized water.

2.2. Cathodes preparation

The raw Ti plates were polished to remove oxide on the surface and subsequent etching was performed in 15% oxalic acid for 2 hours. Then, these plates were washed with deionized water and dried at temperature of 105 °C for 30 min. After the pretreatment, Ti plates were spread with precursor solutions and evaporated at 105 °C for 15 min, and then calcined at 350 °C for 20 min. The above steps were repeated 20 times and finally the electrodes were baked at 350 °C for 2 h.

The precursor solutions were prepared by dissolution of $Cu(NO_3)_2 \cdot 3H_2O$ or $Zn(NO_3)_2 \cdot 6H_2O$ in a hybrid of HNO_3 and ethanol, which maintained HNO_3 at 5% (*w*/*w*) in all precursor solutions. For Ti/CuO_x, Ti/Cu_5ZnO_x and $Ti/CuZn_5O_x$ preparation, the concentration of Cu^{2+} were 0.2, 0.2, 0.04 M, respectively and the concentration of Zn^{2+} ions were 0, 0.04, 0.2 M, respectively.

2.3. Electrochemical set-up

An electrochemical cell with effective volume of 1 L (the cathodic and anodic chambers were 0.7 L and 0.3 L, respectively) was equipped with a cation exchange membrane (CEM, Ultrex CMI-7000). The prepared electrode with dimension of 10cm ×10cm and Ti/RuO_2-IrO_2 (10cm ×10cm) were used as cathode and anode, respectively. The inter-distance of electrodes was 7.5 cm. Two saturated calomel electrodes (SCE) were arranged on surfaces of anode and cathode via Luggin capillary probes in order to record the potential during nitrate reduction.

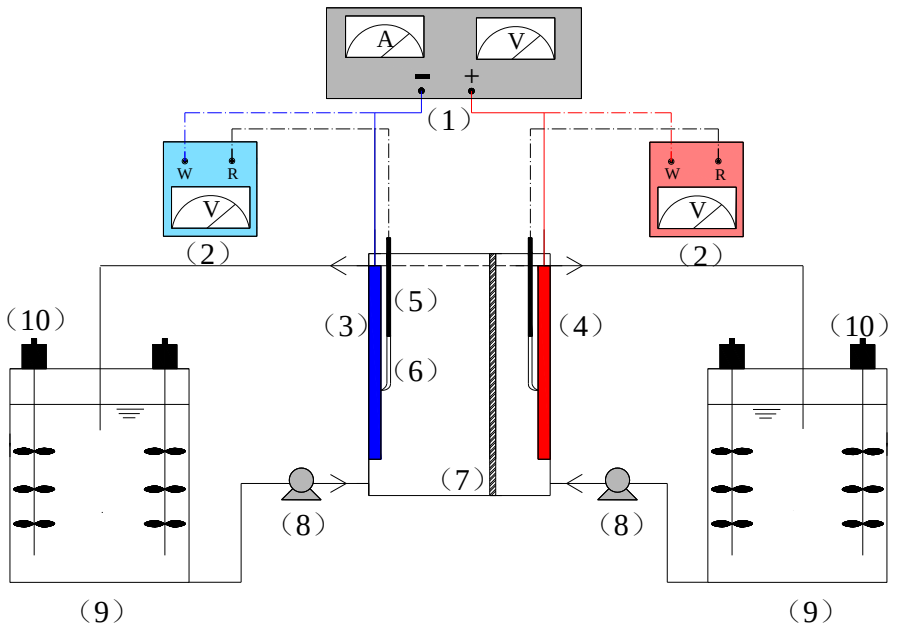

Figure 1. Schematic diagram of the electrochemical apparatus for nitrate cathodic reduction. (1) D.C. power supply; (2) Potentionmeter; (3) Cathode; (4) Anode; (5) SCE; (6) Luggin capillary; (7) Membrane; (8) Peristaltic pump; (9) Reservoir; (10) Stirrer.

The schematic of the set-up used in this study is shown in Fig. 1. The cathodic and anodic solutions were prepared with 150 mg/L $NaNO_3$ and 500 mg/L NaCl, respectively. Na_2SO_4 was employed as support electrolyte and added with dosage of 3% (*w*/*w*). The solutions were pumped into the cell for reaction under a constant flow rate of 150 mL/min by peristalic pumps (Model: BT601F) connected to the water reservoirs (3 L) and the experiments were carried out at room temperature.

2.4. Physic-chemical measurements of the prepared cathodes

The morphology, element composition and atomic ratio of electrodes were detected by a scanning electron microscopy (SEM, FEI Quanta 250, USA) and an energy dispersive spectroscopy (EDS) in conjunction with the SEM, respectively. The X-ray diffraction (XRD) pattern was obtained by using a D8 advance diffractometer (Bruker Corporation, Germany) with a Cu Kα radiation at 40 kV and 30 mA at a scan rate of 0.2°/s and 2θ range of 20° to 90°.

The linear sweep voltammetric (LSV) test was conducted with a three electrode system on a CHI 660E electrochemical workstation by using the prepared cathodes (2cm×2cm), Pt plate (4cm×4cm) and SCE as working, counter and reference electrodes, respectively. Since the nitrate reduction reaction is slightly affected by supporting electrolytes [8], the solutions were composed of 0.1M $NaClO_4$ and various amount of $NaNO_3$ at different pH values (11, 12 and 13) adjusted by NaOH were used to maintain the LSV tests. The investigation was performed between -0.4V and -2.5V (*vs.* SCE) at scan rate of 10 mV/s and the measurements were repeated at least 3 times until a stable one was obtained.

2.5. Analytical methods

The solution pH was determined by a pH-meter (Model: PHSJ-4F, China). The concentrations of NO_3^-, NO_2^- and NH_4^+ in the solution were analyzed according to Standard Methods [25]. The N_2 quantity was achieved through mass balance analysis by assuming that other less quantities of gaseous N-species (e.g. nitrogen oxide, gaseous ammonia) were ignored [13, 20].

The selectivity (S_X, %) and current efficiency (η_X, %) during nitrate reduction could be calculated by Eqs. (1) and (2), respectively

$$S_X = \frac{C_X}{\sum C_X} \times 100 \quad (1)$$

$$\eta_X = \frac{nFC_X}{14It} \times 100 \quad (2)$$

where C_X is the concentration of product X after 6 hours electrolysis (g/L), $\sum C_X$ the sum of quantity of all products (g/L); X depicts NO_2^-, NH_4^+ and N_2; n the number of electron transferred during reactions, F the Faraday constant (96,485 C/mol), 14 the molar mass of nitrogen (g/mol), I the current (A), t the electrolysis time (h). In this work, the η_X values are the total one by considering all products during nitrate degradation.

3. RESULTS AND DISCUSSION

3.1. Physic-chemical characterization of the prepared cathodes

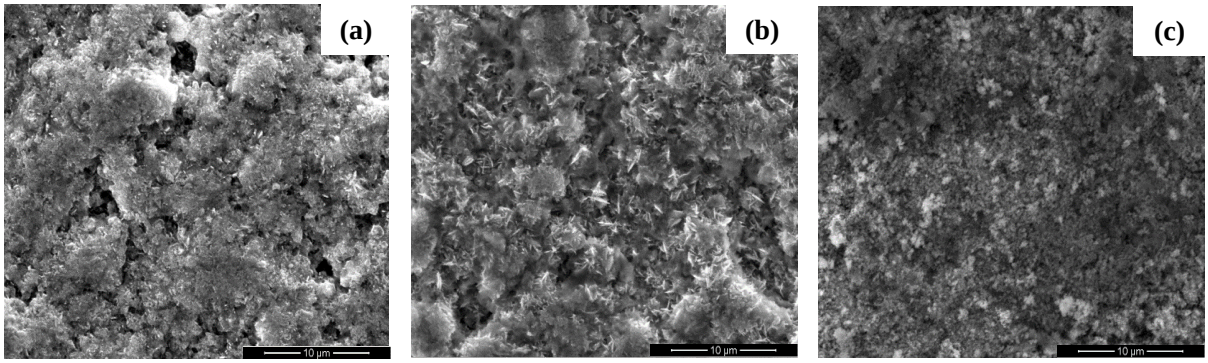

Figure 2. SEM images of the prepared cathodes: Ti/CuO_x (a), Ti/Cu_5ZnO_x (b), Ti/$CuZn_5O_x$ (c).

Table 1. Chemical composition of the different Cu-Zn oxide composite cathodes in this study.

Element	Titanium (at.%)	Oxygen (at.%)	Copper (at.%)	Zinc (at.%)	Cu/Zn (at.%)
Ti/CuO	5.85	58.12	36.03	-	-
Ti/Cu_5ZnO_x	7.07	67.23	21.67	4.03	5.37:1
Ti/$CuZn_5O_x$	1.89	59.14	6.33	32.65	1:5.16

Fig. 2 provides SEM images of the prepared cathodes. Seen from this figure, we can observe the films are in irregular distribution on Ti plates and the surface of the Ti/ Cu_5ZnO_x (Fig. 2b) is covered with class of spicules; this microstructure is favorable to electrode area expansion, leading to increase of reaction kinetics. Table 1 shows the relative atomic percent contents (at. %) of various elements on the surface measured by EDS. It can be demonstrated that Cu/Zn atomic ratios on the surface of Ti/Cu_5ZnO_x and Ti/$CuZn_5O_x$ electrodes were 5.37:1 and 1:5.16, respectively, closed to the theoretical values of precursor added $Cu(NO_3)_2$ and $Zn(NO_3)_2$, indicating that titanium substrate was successfully coated with copper and zinc. Analyzing from the XRD patterns shown in Fig. 3, CuO with crystal phase of tenorite (JCPDS, 45-0937) was detected in the three electrodes, but they also illustrate large difference in the contents: $6CuOCu_2O$ with tetragonal crystal phase (JCPDS, 03-0879) was found in the Ti/CuO_x and Ti/Cu_5ZnO_x electrodes and ZnO with hexagonal crystal phase (JCPDS, 36-1451) was detected in the Ti/$CuZn_5O_x$ cathode. As shown in Table 2, the lattice constants for CuO nanoparticles of these prepared cathodes were calculated from the XRD data. It is easy to find that the lattice constant "a" decrease but "b" "c" increase gradually with the increase of zinc contents on these cathodes, indicating that zinc is beneficial to the change of lattice constant for CuO. In addition, comparing with hexagonal ZnO (JCPDS, 36-1451), the lattice constants of ZnO "a" and "c" decreased from 0.3250nm to 0.3238nm and 0.5207nm to 0.5165nm, respectively, for the Ti/$CuZn_5O_x$ electrode. This can be explained that Cu^{2+} lodges into the position of Zn^{2+} in the Ti/$CuZn_5O_x$ electrode, which

leads to a decrease of the lattice constants as the radius of Cu^{2+}(0.072nm) is smaller comparing with Zn^{2+}(0.074nm) [26]. This change trend of lattice constant possibly implies formation of (Cu-Zn)O solid solution [27, 28].

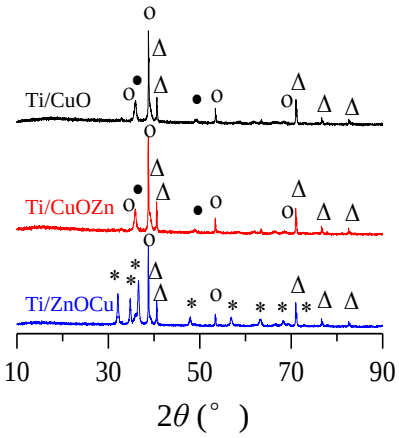

Figure 3. XRD patterns of the cathodes, the symbols of Δ, •, o and * represent the Ti, $6CuOCu_2O$, CuO and ZnO.

Table 2. lattice constant of CuO for the various Cu-Zn oxide composite cathodes.

Element	CuO#45-0937	Ti/CuO	Ti/Cu_5ZnO_x	$Ti/CuZn_5O_x$
a (nm)	0.4685	0.4672	0.4665	0.4664
b (nm)	0.3426	0.3427	0.3431	0.3430
c (nm)	0.5130	0.51268	0.5128	0.5139

The contents of products and current efficiency during nitrate reduction on the Ti/CuO_x, Ti/Cu_5ZnO_x and $Ti/CuZn_5O_x$ cathodes are shown in Fig. 4. This figure illustrates nitrate removals on the three cathodes all increase with enhancement of the current densities and the higher the larger. Minor difference of the nitrate removals of these electrodes are found at lower current density (e.g. 1 or 5 mA/cm^2); but when current density is increased to 20 mA/cm^2, the nitrate removal of Ti/Cu_5ZnO_x is higher than those of other two cathodes, demonstrating the CuO coupling to elemental zinc could effectively accelerate the nitrate removal. These results prove the Cu-Zn oxidize composite cathodes are superior to the metallic alloy electrodes in nitrate degradation reported by other researchers [20, 21]. During nitrate reduction, only a portion of nitrate is reduced to nitrogen gas, the detected NO_2^- and NH_4^+ ions could be formed according to the following equations [29, 30]:

$$NO_3^- (sol) \leftrightarrow NO_3^- (ads) \quad (3)$$

$$NO_3^- (ads) + 2e^- + H_2O \rightarrow NO_2^- (sol) + 2OH^- \quad (4)$$

$$NO_2^- (sol) \leftrightarrow NO_2^- (ads) \quad (5)$$

$$NO_2^- (ads) + 3e^- + 2H_2O \rightarrow 1/2N_2 (g) + 4OH^- \quad (6)$$

$$NO_2^- (ads) + 6e^- + 6H_2O \rightarrow NH_4^+ + 8OH^- \quad (7)$$

Analyzed by the experimental data, we conclude that NO_2^- would not be massively accumulated in the solution regardless of the cathode materials except the lower applied current density (1 mA/cm^2), that is to say, reaction (6) or (7) is a fast one that dominated by reaction (4). However, it is unfortunate that NH4+ selectivity on the three cathodes is much higher than that of N_2, especially on the Ti/$CuZn_5O_x$.

3.2. Electrochemical reduction of nitrate

3.2.1 Products and variation of current efficiency

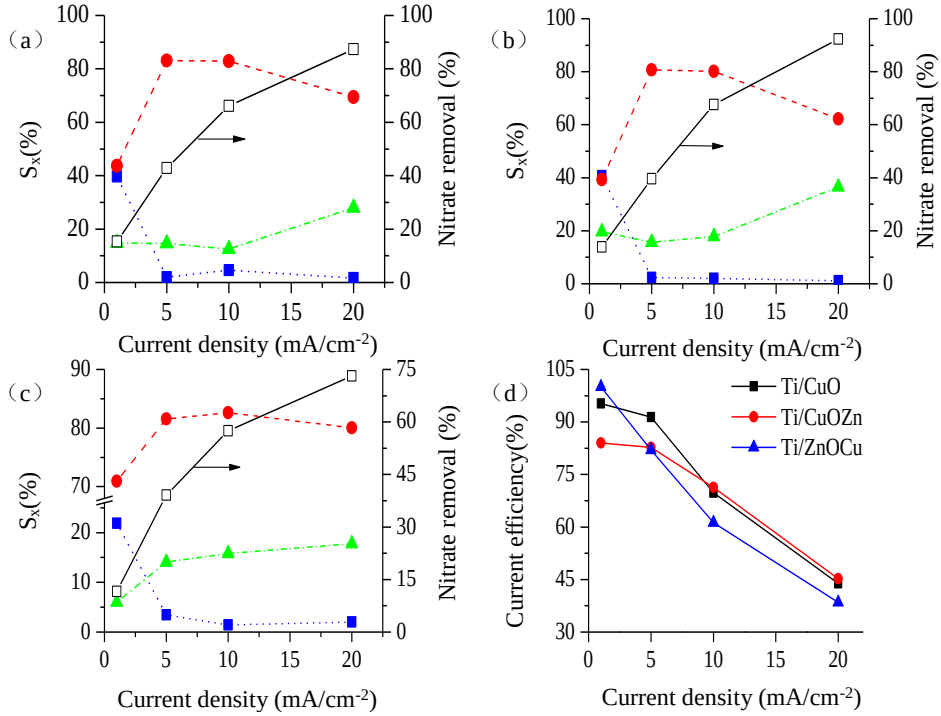

Figure 4. The selectivity of intermediate products on Ti/CuO_x (a), Ti/Cu_5ZnO_x (b) and Ti/$CuZn_5O_x$ (c)cathodes, and current efficiency (d) during nitrate reduction at different applied potentials and reaction time of 6 h. Notations: NO_3^--N(—□—); NO_2^--N(■); NH_4^+-N(●); N_2-N(▲).

It should be pointed out that the ability of complete conversion of nitrate to N_2 is an important index in evaluating the electrode performance and it is interesting that the S_X values of the prepared cathodes are almost in accordance with trends of the nitrate removal. Furthermore, we could observe the N_2 selectivity on Ti/$CuZn_5O_x$ is independent of the current density and the S_X values are very small that remain constant of 14.1%-17.8% at 5 to 20 mA/cm^2. On the contrary, the N_2 production on the Ti/Cu_5ZnO_x and Ti/CuO_x highly relies on the current density and the S_X values abruptly increase from 17.8% and 12.6% to 36.5% and 28.0% at current densities of 10 and 20 mA/cm^2, respectively, which is superior to those of Cu-Zn alloys [20, 21]. On the other hand, the current efficiency of the cathodes decreases with increase of current densities, meaning lower one would be power-saving; but somewhat

incongruously, these two contradictory approaches should be achieved simultaneously by investigating the intrinsic mechanisms of nitrate conversion in detail.

3.2.2 Variation of potentials

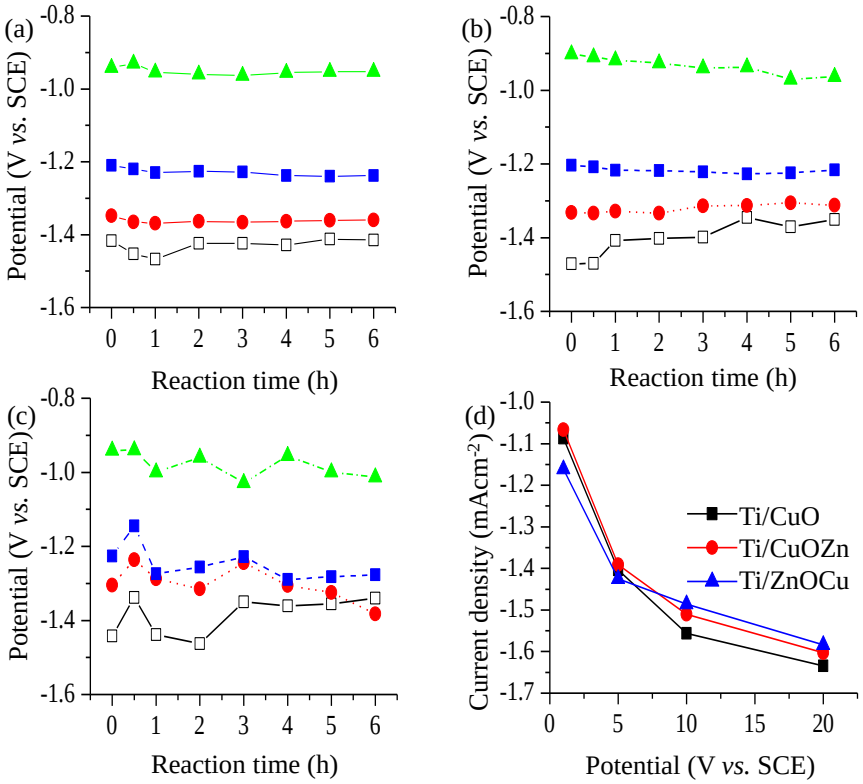

Figure 5. The variation of cathodic potentials on Ti/CuO_x (a), Ti/Cu_5ZnO_x (b) and $Ti/CuZn_5O_x$ (c) cathodes, and relationship between current density and potentials (d) during nitrate reduction in presence of $NaNO_3$ (150 mg/L) and Na_2SO_4 (3% *w/w*). Notations: 1mA/cm^{-2}(▲); 5mA/cm^{-2}(■); 10mA/cm^{-2}(●); 20mA/cm^{-2}(□).

Fig. 5 shows the variation of anodic and cathodic potentials during nitrate reduction with reaction time of 6 h under different operating conditions. As expected, the recorded potentials correspondingly enhance with the increase of current densities. Almost constant potentials on the Ti/CuO_x and Ti/Cu_5ZnO_x cathodes but obviously changed ones on the $Ti/CuZn_5O_x$ are displayed with their respective current densities, implying that the active layer of Ti/CuO_x and Ti/Cu_5ZnO_x is more stable than that of $Ti/CuZn_5O_x$. In addition, we observe from Fig. 5 (d) that the average cathodic potentials of these electrodes are different under a certain current density: the potentials of Ti/Cu_5ZnO_x cathode are always higher than those of Ti/CuO_x at the same current densities, indicating the addition of zinc is beneficial to electron transfer from the electrode surface to aqueous solution; as for the potentials of $Ti/CuZn_5O_x$, they are relatively higher but obviously lower than those of other two electrodes at 10 or 20 mA/cm^2 and 1 or 5 mA/cm^2, respectively, probably attributing to increase of electron transfer via the change of labile ZnO crystal pattern with larger current density and its weak

nitrate reduction capability at a less one. Till date, researchers have revealed that the nitrate reduction highly relies on the cathodic potentials [14, 31]; as a result, LSV test should be further conducted to make clear the intrinsic mechanisms affected by different potentials for nitrate degradation on the prepared electrodes.

3.3. Nitrate reduction mechanisms

3.3.1 LSV analysis at different pH values

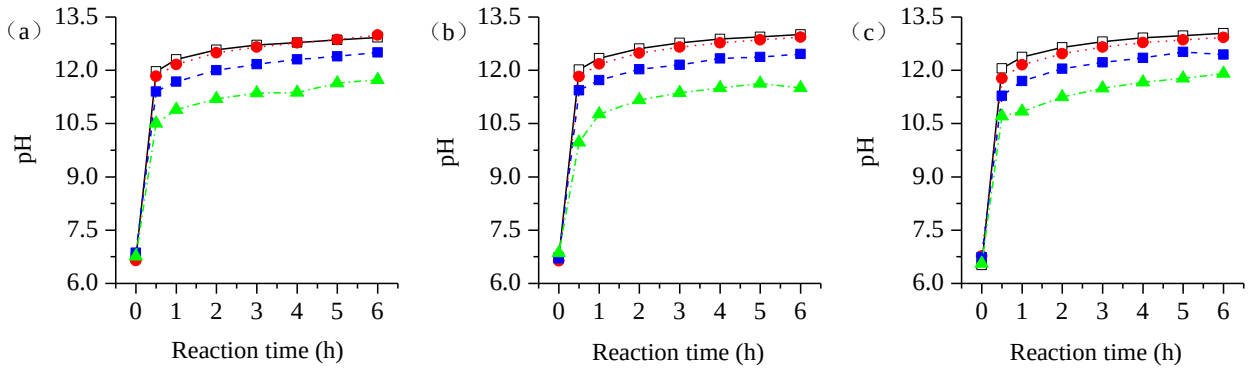

Figure 6. The variation of pH values in cathodic chamber when Ti/CuO_x (a), Ti/Cu_5ZnO_x (b) and Ti/$CuZn_5O_x$ (c) cathodes were employed for nitrate reduction. Notations: 1mA/cm^{-2}(▲); 5mA/cm^{-2}(■); 10mA/cm^{-2}(●); 20mA/cm^{-2}(□).

During nitrate reduction, nitrate ions are firstly absorbed by active sites of the cathodes [32], and the adsorbed hydrogen ions would compete with the main reaction, which maybe decreases the removal efficiency of nitrate in aqueous solution. In this study, we observe from Fig. 6 that the pH values vary from the initial 7.0 to about 11, 12, 13 and 13 at the four current densities on the all prepared cathodes, respectively. Hence, the LSV investigations under pH values of 11, 12 and 13 were conducted to evaluate the effect of the HER on nitrate conversion (Fig. 7). In the blank electrolyte (pH11, 0.1 M $NaClO_4$ only), an obvious downwards trend attributing to the HER is obtained and the potentials of HER are about -1.36 V, -1.50 V and -1.42 V when the Ti/CuO, Ti/Cu_5ZnO_x and Ti/$CuZn_5O_x$ cathodes are employed, respectively. While in presence of the nitrate, the feedback currents obviously rise with increase of alkalinity and the currents of Ti/Cu_5ZnO_x cathode are higher than those of Ti/CuO_x and Ti/$CuZn_5O_x$, indicating Cu_5ZnO_x composite is an excellent candidate for nitrate reduction. We also find the potentials for HER in these solutions are slightly enhanced compared with those obtained in the blank electrolyte, which illustrates hydrogen evolution could be hindered by the nitrate reduction reactions. In an alkaline solution, the HER involves the following major steps:

$$OH^-_{sol} \leftrightarrow OH^-_{ads} \quad (9)$$

$$H_2O_{ads} \leftrightarrow OH^-_{ads} + H^+_{ads} \quad (10)$$

$$H^+_{ads} + e^- \leftrightarrow H_{ads} \quad (11)$$

$$2H_{ads} \leftrightarrow H_2\uparrow \quad (12)$$

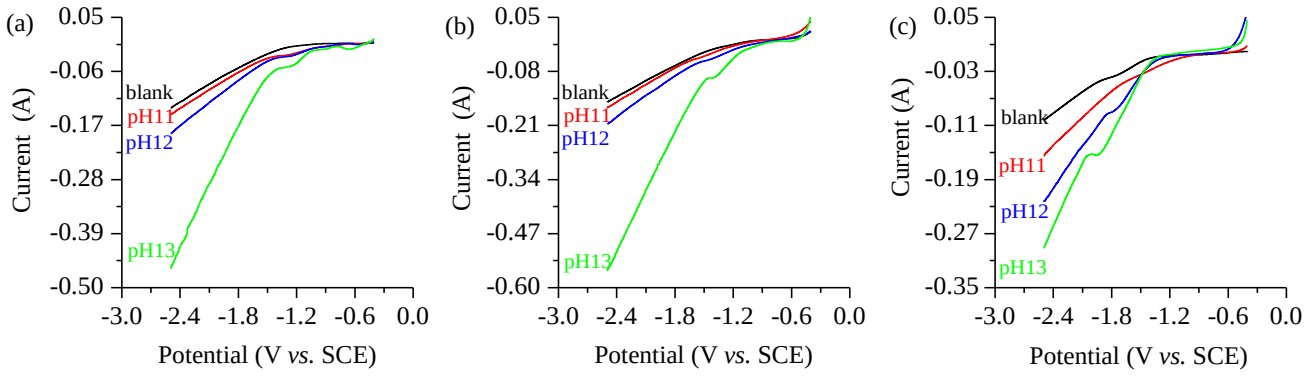

Figure 7. LSVs of the Ti/CuO_x (a), Ti/Cu_5ZnO_x (b) and Ti/$CuZn_5O_x$ (c) cathodes in presence of $NaClO_4$ (0.1 M) and $NaNO_3$ (0.01 M) under different pH values at scanning rate of 10 mV/s.

Thus, a strong bonding and high coverage of OH^-_{ads} (Eq. (9)) restrain selfionization of H_2O_{ads} (Eq. (10)) and decrease the electron-transfer steps (Eqs. (11) and (12)) therefore increase the overpotential for the hydrogen evolution [33]. Furthermore, many distinct reduction peaks are observed at potentials of 0.66V, -0.91V, -1.24V on the Ti/CuO_x and -0.63V, -1.12V, -1.38V on the Ti/Cu_5ZnO_x electrodes (pH13), respectively. These facts depict that the presence of OH^- ions induce, to some extent, an inhibition of hydrogen ions adsorption thereby to increase the N-species adsorption on the surface of these cathodes.

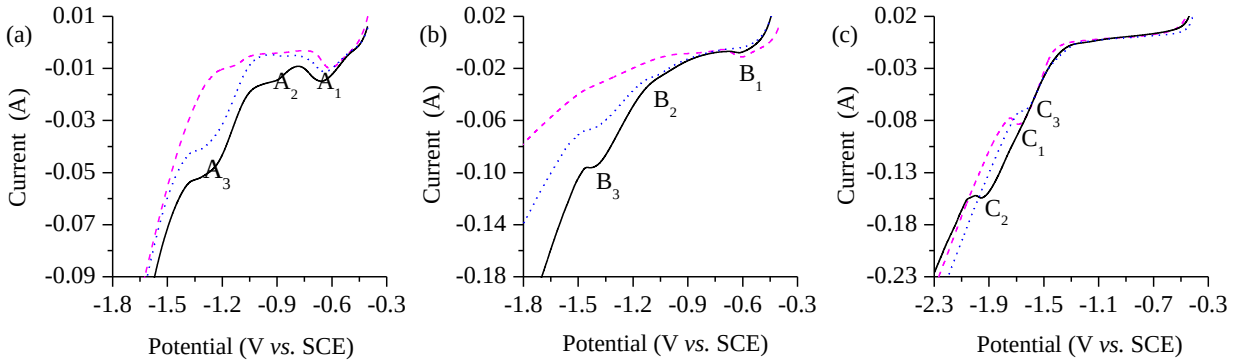

Figure 8. LSVs of the Ti/CuO_x (a), Ti/Cu_5ZnO_x (b) and Ti/$CuZn_5O_x$ (c) cathodes at pH 13 in aqueous solutions containing 0.1M $NaClO_4$(· · ·), and added 0.01M $NaNO_3$(——) or 0.01M $NaNO_2$ (- - -) at scanning rate of 10 mV/s.

Aiming to determine the mechanisms of nitrate reduction on the prepared three cathodes, LSV tests were further carried out in aqueous solutions of $NaClO_4$, $NaNO_3$ and $NaNO_2$ at pH 13 and the results are described by Fig. 8. As shown in Fig. 8a, the data obtained in nitrate electrolyte presents three reduction peaks at potentials of -0.66V (A_1), -0.91V (A_2) and -1.24V (A_3) prior to occurrence of the HER. Less feedback currents are observed when nitrite solution is used, and we also can assert the A_2 peak is associated with the reduction of nitrate to nitrite ions from the disappearance of this peak. Comparison of these curves with that achieved in $NaClO_4$ solution, it could be ensured that the A_3 and A_1 peaks should be related to nitrite reduction (Eqs. (6) and (7)) and CuO conversion, respectively. The similar phenomena for nitrate reduction obtained in alkaline solution on copper cathode were

previously reported by Reyter et al. [14] and Mattarozzi et al. [18]. The LSVs of Ti/Cu_5ZnO_x cathode behave the same shape to those of Ti/CuO_x but potentials for the three peaks shift to -0.60V (B_1), -1.07V (B_2), -1.41V (B_3), respectively. It can be observed that the reduction potentials of nitrate to nitrite and nitrite further degradation on Ti/CuO_x (Cu=36.0 at. %) are more positive than those on Ti/Cu_5ZnO_x (Cu=21.7 at. %). This is probably because more copper could accelerate the adsorption of NO_3^- ions by retarding hydrogen ions transfer therefore enhancing the conversion of NO_3^- to NO_2^- ions, which is in accordance with the published works [9]. However, relatively less feedback currents in nitrite solution comparing with those in nitrate electrolyte both on Ti/CuO_x and Ti/Cu_5ZnO_x cathodes are found, indicating copper has a negative effect in the degradation activity and selectivity of NO_2^- to N_2. When the $Ti/CuZn_5O_x$ cathode is employed, not any reduction peak for nitrate degradation is captured by the LSV investigation, but a new peak or wave arises in each LSVs after the HER (Fig. 8c). The existence of wave C_1 in blank electrolyte over potential region of -1.58 V to -1.70 V is due to the H-poisoning on the electrode surface by adsorbed hydrogen, blocking the nitrate reduction process [14, 18]. The shift of wave C_2 to more negative potential region of -1.9 V to -2.0 V in presence of nitrate ions indicates the inhibition of the H-poisoning by nitrate reduction. Furthermore, the detection of an even more positive wave C_3 by the H-poisoning in presence of NO_2^- ions reflects a much less effective reactivity than that in NO_3^- ions.

The LSVs under different conditions demonstrate the nitrate reduction could be effectively conducted in alkaline solution on the prepared electrodes and the Ti/Cu_5ZnO_x cathode possesses higher reduction ability in comparison with the others, which also could be confirmed by the electrochemical reduction of nitrate shown in Figs. 4 to 6.

3.3.2 Degradation rate of nitrate

According to published literature [15], the nitrate reduction is assumed as first-order kinetics and the relation between current density and nitrate concentration can be described by the following equation:

$$\log j_{E_x} = \log k + n \log[NO_3^-] \quad (13)$$

where j_{Ex} is the current density at potential E_x, k the rate constant, n the reaction order and $[NO_3^-]$ the nitrate concentration. Hence, k values of the Ti/CuO, Ti/Cu_5ZnO_x and $Ti/CuZn_5O_x$ cathodes at pH 11, 12 and 13 could be calculated by the current density corresponding to their respective potentials under different nitrate concentrations and the results are displayed in Fig. 9. The rate constants for nitrate conversion on the Ti/Cu_5ZnO_x electrode increase with enhancement of the pH values and potentials, and the increase is more remarkable at a higher alkaline solution. Similarly, an increasing electroactivity of $Ti/CuZn_5O_x$ is also shown, but the change is much less than those of Ti/Cu_5ZnO_x. As for the Ti/CuO_x one, whatever the potentials, it possesses excellent electroactivity of nitrate reduction at pH 11, however, the excellent activity is not significantly improved with variations of solution pH at higher potentials (E_3 or E_4), which may seem inconsistent with change rules of k value of the cathodes containing zinc.

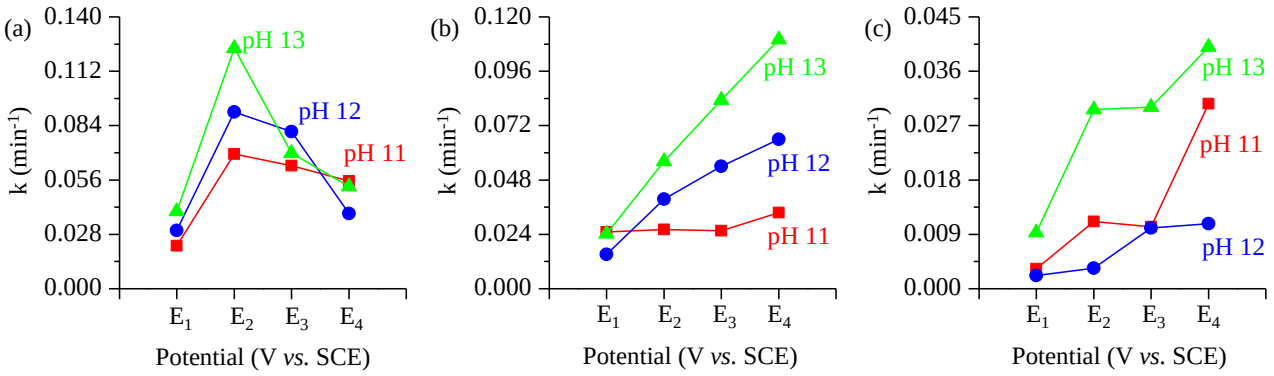

Figure 9. The apparent rate constants of the Ti/CuO_x (a), Ti/Cu_5ZnO_x (b) and Ti/$CuZn_5O_x$ (c) cathodes at their respective potentials(E_1, E_2, E_3, E_4 corresponding to current densities of 1, 5, 10 and 20 mA/cm^2).

3.3.3 Degradation mechanisms of nitrate

Based on the above analysis, one can conclude that the copper oxide is active for initial adsorption of nitrate and electron transfer due to the higher nitrate degradation on Ti/CuO_x cathode prior to the HER (Fig. 4) and the accumulation of OH^- in aqueous solution could weaken H_{ads} occupation on electrode surface thereby free more active sites for nitrate adsorption under this condition. On the contrary, more negative potentials may benefit the H_{ads} adsorption on the surface of CuO after the HER, resulting into a constant pH values during nitrate reduction (Fig. 6).

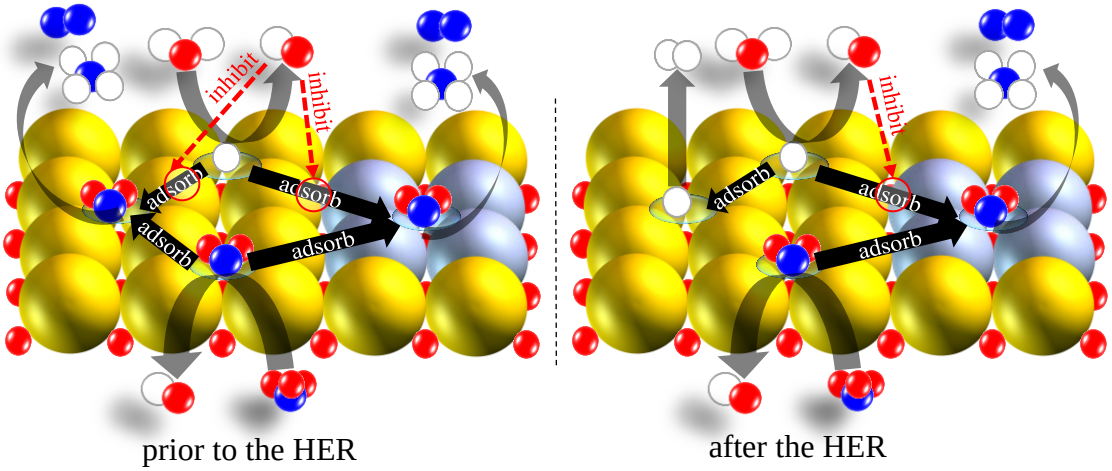

Figure 10. The mechanism for activity and selectivity in alkaline electrolytes for Cu-Zn mixed cathodes. Yellow, gray, red, blue and white atoms represent Cu, Zn, O, N and H atoms, respectively.

As a contrast, Ti/Cu_5ZnO_x electrode could always reduce H_{ads} adsorption at a wide potential window and the increasing electroactivity of nitrate reduction after the HER should be related to the existence of zinc element. It can be inferred that zinc is to offer active sites for intermediate N-species degradation, especially in a high alkaline solution and this effect to some extent benefit for complete

reduction of nitrite to N_2, confirming by higher selectivity of N_2 generation on containing-zinc cathodes (Ti/Cu_5ZnO_x and Ti/$CuZn_5O_x$) comparing with on non-zinc cathode(Ti/CuO_x). The proposed reaction mechanism to describe the activity and selectivity of the Cu-Zn oxidize composite cathodes in alkaline electrolytes is presented in Fig. 10.

It is worth to be noted that Cu element shows a negative influence on activity and selectivity for nitrite degradation and rare element (Pd) is necessary to be required to offer active sites for production of the intermediate products, such as NO_2^-, NO and N_2O to N_2 [8, 9], which makes the nitrate removal extremely expensive. Interestingly, almost the same performance to those rare metals is also achieved by the prepared Cu-Zn oxidize composite cathodes and hence this work provides a low-cost strategy for effective nitrate reduction.

4. CONCLUSIONS

This study investigated the electroreduction of nitrate by using different prepared cathodes (Ti/CuO, Ti/Cu_5ZnO_x and Ti/$CuZn_5O_x$). The following conclusions can be drawn: (1) Cu-Zn oxide composite can be bound together by thermal decomposition method and active CuO nanoparticles were more stable than other metal oxides in the process of nitrate reduction; (2) Ti/Cu_5ZnO_x cathode exhibits higher activity in nitrate removal and considerable selectivity of N_2 production, and ammonium ion is the main product on the three electrodes; (3) the presence of OH^- ions enhanced electroactivity of the Ti/Cu_5ZnO_x and Ti/$CuZn_5O_x$ cathodes, especially after the HER, and the zinc element could provide extra active sites for intermediate N-species reduction via inhibition of adsorbed hydrogen ion.

ACKNOWLEDGEMENT
This work was financially supported by the Fundamental Research Funds for the Central Universities of China (2015XKZD10).

References

1. S.R. Carpenter., N.F. Caraco., D.L. Correll., R.W. Howarth., A.N. Sharpley., V.H. Smith., *Ecol. Appl.*, 8 (1998) 559.
2. M.H. Ward, T.M. deKok, P. Levallois, J. Brender, G. Gulis, B.T. Nolan, J. VanDerslice, *Environ. Health Persp.*, 113 (2005) 1607.
3. S. Ghafari, M. Hasan, M.K. Aroua, *Bioresource technol.*, 99 (2008) 3965.
4. T. Kikhavani, S.N. Ashrafizadeh, B. Van der Bruggen, *Electrochim. Acta*, 144 (2014) 341.
5. R. Epsztein, O. Nir, O. Lahav, M. Green, *Chem. Eng. J.*, 279 (2015) 372.
6. W.B. Li, Y.B. Song, H.K. Xu, L.Y. Chen, W.H. Dai, M. Dong, *Environ. Sci. Pollut. R.*, 22 (2015) 9575.
7. P.M. Tucker, M.J. Waite, B.E. Hayden, *J. Appl. Electrochem.*, 34 (2004) 781.
8. A.C.A. de Vooys, R.A. van Santen, J.A.R. van Veen, *J. Mol. Catal. A-Chem.*, 154 (2000) 203.
9. L. Szpyrkowicz, S. Daniele, M. Radaelli, S. Specchia, *Appl. Catal. B-Environ.*, 66 (2006) 40.
10. M. Li, C. Feng, Z. Zhang, N. Sugiura, *Electrochim. Acta*, 54 (2009) 4600.

11. I. Katsounaros, D. Ipsakis, C. Polatides, G. Kyriacou, *Electrochim. Acta*, 52 (2006) 1329.
12. I. Katsounaros, G. Kyriacou, *Electrochim. Acta*, 52 (2007) 6412.
13. J. Ding, W. Li, Q.-L. Zhao, K. Wang, Z. Zheng, Y.-Z. Gao, *Chem. Eng. J.*, 271 (2015) 252.
14. D. Reyter, D. Bélanger, L. Roué, *Electrochim. Acta*, 53 (2008) 5977.
15. D. Reyter, D. Belanger, L. Roue, *J. Hazard. Mater.*, 192 (2011) 507.
16. D. Pletcher, Z. Poorabedi, *Electrochim. Acta*, 24 (1979) 1253.
17. V. Rosca, M. Duca, M.T. de Groot, M.T.M. Koper, *Chem. Rev.*, 109 (2009) 2209.
18. L. Mattarozzi, S. Cattarin, N. Comisso, P. Guerriero, M. Musiani, L. Vázquez-Gómez, E. Verlato, *Electrochim. Acta*, 89 (2013) 488.
19. Z. Mácová, K. Bouzek, J. Šerák, *J. Appl. Electrochem.*, 37 (2007) 557.
20. N. Fan, Z. Li, L. Zhao, N. Wu, T. Zhou, *Chem. Eng. J.*, 214 (2013) 83.
21. M. Li, C. Feng, Z. Zhang, Z. Shen, N. Sugiura, *Electrochem. Commun.*, 11 (2009) 1853.
22. E.V. Filimonov, A.I. Shcherbakov, *Prot. Met.*, 40 (2004) 280.
23. M. Sakai, Y. Nagai, Y. Aoki, N. Takahashi, *Appl. Catal. A-Gen.*, 510 (2016) 57.
24. A. Patel, P. Shukla, J. Chen, T.E. Rufford, V. Rudolph, Z. Zhu, *Catal. Today*, 212 (2013) 38.
25. APHA, Standard methods for the examination of water and wastewater (22nd ed.), American Water Works Association, (2012) Washington, America.
26. H. Li, Y. Zhang, X. Pan, H. Zhang, T. Wang, E. Xie, *J. Nanopart. Res.* 11 (2008) 917.
27. I.A. Mudunkotuwa, J.M. Pettibone, V.H. Grassian, *Environmen. Sci. Technol.*, 46 (2012) 7001.
28. C.C. Vidyasagar, Y.A. Naik, T.G. Venkatesh, R. Viswanatha, *Powder Technol.*, 214 (2011) 337.
29. H. Shin, S. Jung, S. Bae, W. Lee, H. Kim, *Environ. Sci. Technol.*, 48 (2014) 12768.
30. J. Jung, S. Bae, W. Lee, *Appl. Catal. B-Environ.*, 127 (2012) 148.
31. J.F. Su, I. Ruzybayev, I. Shah, C.P. Huang, *Appl. Catal. B-Environ.*, 180 (2016) 199.
32. M.S. El-Deab, *Electrochim. Acta*, 49 (2004) 1639.
33. D. Reyter, D. Belanger, L. Roue, *Water res.*, 44 (2010) 1918.